13th International Conference on
Steel, Space and Composite Structures
31 January - 2 February 2018, Perth, Australia

MULTI-SCALE MODELLING OF TIME-DEPENDENT RESPONSE OF COMPOSITE STRUCTURES MADE OF ORTHOTROPIC VISCOELASTIC MATERIALS

Sardar Malek[*], Thomas Gereke[†], Nima Zobeiry[‡], and Reza Vaziri[§]

*School of Civil and Environmental Engineering
University of Technology Sydney, Ultimo, NSW, Australia
e-mail: sardar.malek@uts.edu.au

Keywords: Composites, Multi-scale Modelling, Finite Element Method, Viscoelasticity

Abstract. *Modern structural composites such as advanced fibre-reinforced and strand-based composites are increasingly being used in the new generation of aerospace, automotive, marine and civil engineering structures. To analyse the time-dependent response of these orthotropic composites, an efficient and easy-to-implement approach in the context of 3-D multi-scale modelling, is presented. The modelling approach is based on computational homogenization technique and differential form of viscoelasticity proposed recently for modelling the response of isotropic and transversely isotropic materials. The finite element analyses will be conducted at different length scales in a general purpose finite element code, ABAQUS®. Although the modelling approach is general, it is specifically applied to predict the time-dependent behaviour of a special structural wood composite product, parallel strand lumber (PSL) beam, subjected to a three-point bending load. The effect of microstructural parameters (e.g. wood strand size and orientation distribution, as well as resin area coverage, volume fraction and relaxation modulus) on the creep response of PSL will be demonstrated.*

1 INTRODUCTION

Composite materials with various microstructures and properties are increasingly being developed to meet the needs of design engineers in various industries. Having predictive tools which are capable of relating the material properties at different scales to structural response of composites under complex loading conditions would enable us to accelerate the development of novel composite materials for structural applications.

Analytical micromechanics equations are currently available and used with great success for predicting the effective elastic properties of the solid unidirectional circular fibre composites as well as rectangular strand or veneer-based wood composites. However, their application in predicting the effective viscoelastic properties of composite or cases where one phase could become softer (e.g. due to temperature increase) than the other phase has not been investigated fully. Woven composites and strand-based composites where the fibre (strand) has a rectangular cross-section are examples of such composites. Most of these composite materials show directionally-dependent (orthotropic) properties which make their structural analysis complex. To predict the structural

[†] TU Dresden, Institute of Textile Machinery and High Performance Material Technology, Dresden, Germany
[‡] SNC-Lavalin, Toronto, ON, Canada
[§] Department of Civil Engineering, The University of British Columbia, Vancouver, BC, Canada

response of composites exhibiting time-dependent characteristics special treatment of constitutive models is required.

Several multi-scale models have been developed to take into account the hierarchical nature of composites and solving problems arising from the complex microstructure of new composites. The concept of multi-scale modelling, its origins, recent developments and current challenges in this field have been discussed in several research papers [1], [2]. Currently, multi-scale modelling is a well-established approach in literature for analysing composite materials. However, a multi-scale approach still needs to be efficient enough to be employed for analysing the behaviour of large composite structures in practice. Efficiency becomes a particularly important issue in those applications where time-dependent (viscoelastic) response of the structure is of interest such as process modelling or predicting the long-term behaviour (creep) of structural elements made of new composites. In addition to the efficiency requirement for a multi-scale modelling tool, accuracy is also important for new composites with directionally dependent (orthotropic) properties that are being developed for aerospace and construction application. To address the above requirements, an efficient multi-scale modelling strategy which relates microstructural parameters (e.g. strand size and orientation) to the time-dependent response (e.g. creep) of composite structures is presented below.

2 MODELLING FRAMEWORK

The multi-scale approach presented in this paper is based on other well-established approaches and models and involves analyses at two major resolution levels; namely, micro-level and macro-level as depicted in Figure 1 for modelling the response of parallel strand lumber (PSL) to a constant load. It should be noted that throughout this paper, the macro-scale is the scale at which we are interested in determining the structural response. Scales below the macro-scale such as the meso- and micro-scale may be identified for different composites. Lower scales, in general, are referred to as micro-scale unless stated otherwise.

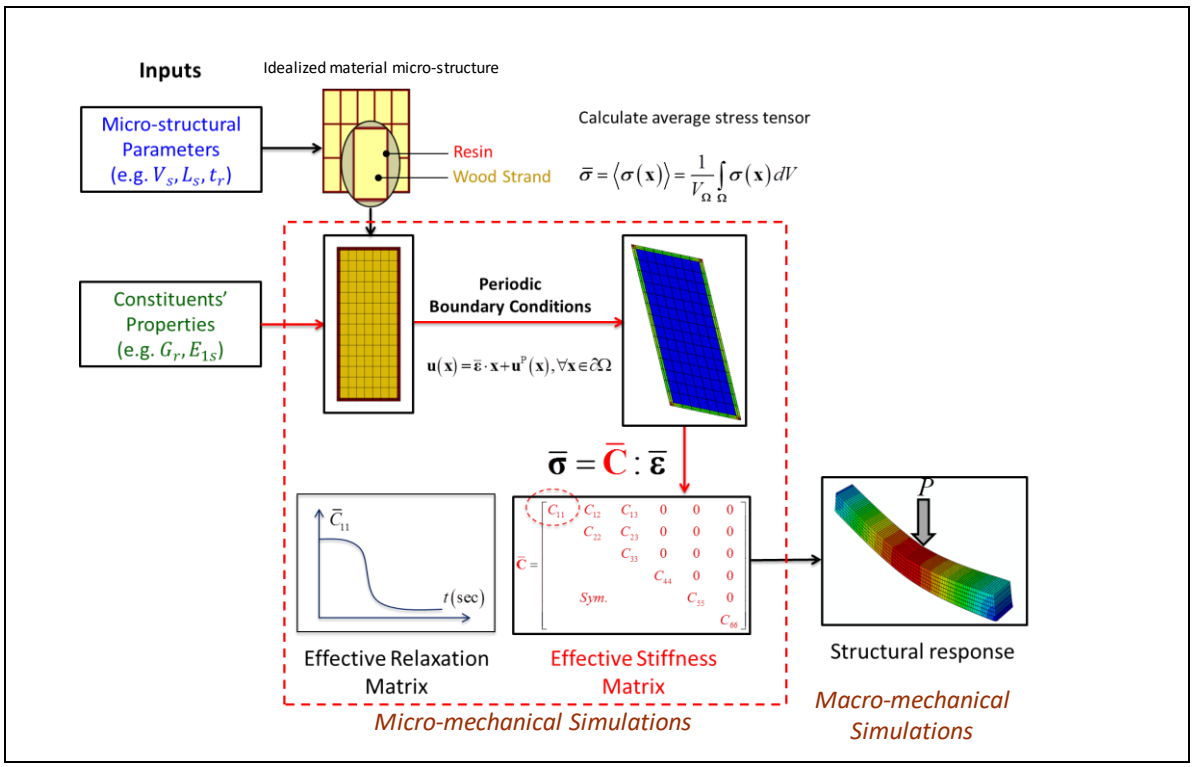

Figure 1: Schematic of the multi-scale modelling approach for simulating the structural behaviour of PSL

3 MICRO-SCALE ANALYSIS

As a first step in multi-scale modelling of viscoelastic composites, the effective viscoelastic properties of composites through a micro-scale analysis is required. The viscoelastic properties of the material unit cell can be estimated analytically using the correspondence principle employed by most researchers, e.g. see [3]–[5]. Using the correspondence principle, the linear viscoelastic heterogeneous problem in the real time domain is first transformed to a virtual linear elastic problem in Laplace space. The latter is then solved using linear micromechanical schemes. Finally, the effective viscoelastic properties are obtained using numerical inversion to time domain.

As an alternative to the analytical approach, the effective viscoelastic behaviour of a unit cell of material can be obtained numerically using finite element method. Assuming a periodic microstructure for the materials, a unit cell of the material can be identified. This unit cell is subjected to six elementary loads which are held constant during time. Components of the effective stiffness tensor are determined during time using the volume average stress and strain tensors at each time step. Therefore, the stiffness tensor components are functions of time and each component can be expressed as a set of continuous mathematical functions, known as Prony series.

4 MACRO-SCALE ANALYSIS

A differential form (DF) of viscoelasticity has recently been presented by Zobeiry and others [6], [7] as an efficient approach for modelling the response of polymer composite materials. The formulations in [6] were developed for transversely isotropic materials and extended by Malek [8] for modelling viscoelastic behaviour of orthotropic composites. The 3-D formulation for orthotropic viscoelastic materials presented in [8] can be easily implemented in virtually any existing code. To illustrate this, such formulation is briefly reviewed here. A user material subroutine (UMAT) has been developed and implemented in the ABAQUS® software. The implementation of the formulation has been verified and presented here through a benchmark example.

4.1 Differential Approach to Modelling Generally Orthotropic Materials

In a general 3-D state of stress, the constitutive equation relating the stress σ_{ij} and the strain ϵ_{ij} for a linear elastic material can be written as follows:

$$\sigma_{ij} = C_{ijkl}\varepsilon_{kl} \tag{1}$$

where C_{ijkl} are components of the material stiffness tensor. Using matrix notation, the stiffness tensor can also be written in a 6 × 6 matrix form, denoted by the symbol $\underline{\underline{C}}$ with the double underscore indicating matrix quantities and single underscore denoting vectors.

For an isotropic material, the stiffness matrix can be expressed in terms of two independent constants (moduli), G and K, representing the shear and bulk behaviour of the material. Therefore, the stress-strain relationship can also be written as follows:

$$\underline{\sigma} = G\begin{Bmatrix} \frac{2}{3}(2\varepsilon_{11}-\varepsilon_{22}-\varepsilon_{33}) \\ \frac{2}{3}(2\varepsilon_{22}-\varepsilon_{11}-\varepsilon_{33}) \\ \frac{2}{3}(2\varepsilon_{33}-\varepsilon_{11}-\varepsilon_{22}) \\ 2\varepsilon_{12} \\ 2\varepsilon_{13} \\ 2\varepsilon_{23} \end{Bmatrix} + K\begin{Bmatrix} \varepsilon_{11}+\varepsilon_{22}+\varepsilon_{33} \\ \varepsilon_{11}+\varepsilon_{22}+\varepsilon_{33} \\ \varepsilon_{11}+\varepsilon_{22}+\varepsilon_{33} \\ 0 \\ 0 \\ 0 \end{Bmatrix} \tag{2}$$

In other words, the total stress vector for an isotropic material can be decomposed into two vectors:

$$\underline{\sigma} = \underline{\sigma}_G + \underline{\sigma}_K \tag{3}$$

where the vectors $\underline{\sigma}_G$ and $\underline{\sigma}_K$, epresent the shear and bulk components of the total stress, respectively. In order to describe the behaviour of an elastic, orthotropic material, nine constants are needed and the stress-strain relationship can be expressed in terms of these nine constants (stiffness

matrix components) as follows:

$$\underline{\underline{\sigma}} = C_{11}\underline{\underline{\varepsilon}}_{C_{11}} + C_{22}\underline{\underline{\varepsilon}}_{C_{22}} + C_{33}\underline{\underline{\varepsilon}}_{C_{33}} + C_{44}\underline{\underline{\varepsilon}}_{C_{44}} + C_{55}\underline{\underline{\varepsilon}}_{C_{55}} + C_{66}\underline{\underline{\varepsilon}}_{C_{66}} + C_{12}\underline{\underline{\varepsilon}}_{C_{12}} + C_{13}\underline{\underline{\varepsilon}}_{C_{13}} + C_{23}\underline{\underline{\varepsilon}}_{C_{23}} \tag{4}$$

where the stress tensor has been decomposed into nine tensors each corresponding to a stiffness matrix component or a material property, p:

$$\underline{\underline{\sigma}} = \underline{\underline{\sigma}}_{C_{11}} + \underline{\underline{\sigma}}_{C_{22}} + ... + \underline{\underline{\sigma}}_{C_{23}} = \sum_{p=1}^{9} \underline{\underline{\sigma}}_{p} \tag{5}$$

For simplicity, the above equation may also be written in vector form as:

$$\begin{aligned}
\underline{\sigma} = \begin{Bmatrix} \sigma_{11} \\ \sigma_{22} \\ \sigma_{33} \\ \sigma_{12} \\ \sigma_{13} \\ \sigma_{23} \end{Bmatrix} &= C_{11}\begin{Bmatrix} \varepsilon_{11} \\ 0 \\ 0 \\ 0 \\ 0 \\ 0 \end{Bmatrix} + C_{22}\begin{Bmatrix} 0 \\ \varepsilon_{22} \\ 0 \\ 0 \\ 0 \\ 0 \end{Bmatrix} + C_{33}\begin{Bmatrix} 0 \\ 0 \\ \varepsilon_{33} \\ 0 \\ 0 \\ 0 \end{Bmatrix} \\
&+ C_{44}\begin{Bmatrix} 0 \\ 0 \\ 0 \\ 2\varepsilon_{12} \\ 0 \\ 0 \end{Bmatrix} + C_{55}\begin{Bmatrix} 0 \\ 0 \\ 0 \\ 0 \\ 2\varepsilon_{13} \\ 0 \end{Bmatrix} + C_{66}\begin{Bmatrix} 0 \\ 0 \\ 0 \\ 0 \\ 0 \\ 2\varepsilon_{23} \end{Bmatrix} \\
&+ C_{12}\begin{Bmatrix} \varepsilon_{22} \\ \varepsilon_{11} \\ 0 \\ 0 \\ 0 \\ 0 \end{Bmatrix} + C_{13}\begin{Bmatrix} \varepsilon_{33} \\ 0 \\ \varepsilon_{11} \\ 0 \\ 0 \\ 0 \end{Bmatrix} + C_{23}\begin{Bmatrix} 0 \\ \varepsilon_{33} \\ \varepsilon_{22} \\ 0 \\ 0 \\ 0 \end{Bmatrix}
\end{aligned} \tag{6}$$

For a viscoelastic orthotropic material, similar to the isotropic or transversely isotropic case in [6], a differential equation is employed to relate the associated stresses and strains as follows:

$$\dot{\underline{\sigma}}_P = P^u \dot{\underline{\varepsilon}}_P - \sum_{i=1}^{N} \frac{1}{(\tau_P)_i}(\underline{\sigma}_P)_i; \qquad P = C_{11}, C_{22}, ..., C_{23} \tag{7}$$

In deriving the above equation, for each component of the stiffness matrix (e.g. C_{11}) a generalized Maxwell model has been employed. For each element i of the generalized Maxwell model a governing differential equation can be written as follows:

$$(\dot{\underline{\sigma}}_P)_i = P^i \dot{\underline{\varepsilon}}_P - \frac{1}{(\tau_P)_i}(\underline{\sigma}_P)_i; \qquad P = C_{11}, C_{22}, ..., C_{23} \tag{8}$$

In the above equation, the spring stiffness and time constant of Maxwell element i associated with component P of the stiffness matrix are denoted by P^i and $(\tau_P)_i$, respectively. The unrelaxed values of each component of stiffness matrix, denoted by superscript u, is obtained by summing over all Maxwell elements. Therefore, the unrelaxed value of component P is obtained as:

$$P^u = \sum_{i=1}^{N} P^i; \qquad P = C_{11}, C_{22}, ..., C_{23} \tag{9}$$

where N is the number of Maxwell elements.

The overall governing differential equation is obtained by summing over all nine stress vectors,

therefore the overall governing differential equation can be written as:

$$\dot{\underline{\sigma}} = \underline{\underline{C}}^{u}\,\dot{\underline{\varepsilon}} - \sum_{P}\sum_{i=1}^{N}\frac{1}{\left(\tau_P\right)_i}\left(\underline{\sigma}_P\right)_i \tag{10}$$

4.2 Implementation

Rewriting Equation (8) at time steps n and $n+1$ for element i of the generalized Maxwell model, including the free strain $\underline{\epsilon}_{pf}$ (e.g. strain generated due to cure shrinkage or thermal expansion) leads to:

$$\begin{cases} \left(\dot{\underline{\sigma}}_P\right)_i^{n} = P^i\left(\dot{\underline{\varepsilon}}_P^{n} - \dot{\underline{\varepsilon}}_{Pf}^{n}\right) - \dfrac{1}{\left(\tau_P\right)_i^{n}}\left(\underline{\sigma}_P\right)_i^{n} \\ \left(\dot{\underline{\sigma}}_P\right)_i^{n+1} = P^i\left(\dot{\underline{\varepsilon}}_P^{n+1} - \dot{\underline{\varepsilon}}_{Pf}^{n+1}\right) - \dfrac{1}{\left(\tau_P\right)_i^{n+1}}\left(\underline{\sigma}_P\right)_i^{n+1} \end{cases} \tag{11}$$

As it is described Zobeiry et al. (2016), using the finite difference method with a central difference scheme and rearranging, the stresses in each Maxwell element "i" can be calculated as:

$$\left(\underline{\sigma}_P\right)_i^{n+1} = \left(\frac{1-\dfrac{1}{2}\dfrac{\Delta t}{\left(\tau_P\right)_i^{n}}}{1+\dfrac{1}{2}\dfrac{\Delta t}{\left(\tau_P\right)_i^{n+1}}}\right)\left(\underline{\sigma}_P\right)_i^{n} + \frac{P^i}{\left(1+\dfrac{1}{2}\dfrac{\Delta t}{\left(\tau_P\right)_i^{n+1}}\right)}\left[\left(\underline{\varepsilon}_P^{n+1} - \underline{\varepsilon}_P^{n}\right) - \left(\underline{\varepsilon}_{Pf}^{n+1} - \underline{\varepsilon}_{Pf}^{n}\right)\right] \tag{12}$$

The total stress vector at time increment $(n+1)$ can be calculated by summing over all Maxwell elements $(i = 1, 2, 3, \ldots, N)$ and material properties P, as follows:

$$\underline{\sigma}^{n+1} = \sum_{P}\sum_{i=1}^{N}\left(\underline{\sigma}_P\right)_i^{n+1}; \qquad P = C_{11}, C_{22}, \ldots., C_{23} \tag{13}$$

Details of the finite element formulation and solution convergence conditions could be found in previous publications of the authors (e.g. [6], [7]).

4.3 Verification example

To verify the implementation of the DF formulations, numerical results are compared with available analytical solutions for a simple example here. The example is taken from [9], in which an orthotropic rectangular rod is subjected to an applied uniaxial stress in the 1-direction prescribed as:

$$\sigma\left(t\right) = \frac{t}{1000}, \quad 0 \le t \le 1000 \tag{14}$$

The viscoelastic properties of the orthotropic material are given in Table 1.

Property	$C_{ij}{}^{g}$ (GPa)	$C_{ij}{}^{r}$ (GPa)	τ_k (s)
C_{11}	3.857	0.319	0.100
C_{22}	3.705	0.303	0.090
C_{33}	3.582	0.291	0.080
C_{44}	2.000	0.160	0.100
C_{55}	1.800	0.150	0.090
C_{66}	1.600	0.140	0.080
C_{12}	1.674	0.139	0.100
C_{13}	1.659	0.137	0.100
C_{23}	1.614	0.291	0.100

Table 1: Viscoelastic properties of the orthotropic material taken from [9].

The variations of non-zero strain components are plotted in Figure 2. In this figure, the analytical solutions have been obtained using Laplace transform and shown with solid lines. The numerical predictions, depicted with symbols, show very good agreement with analytical exact results in all three directions. This validates the capabilities of differential form of viscoelasticity in modelling orthotropic viscoelastic materials.

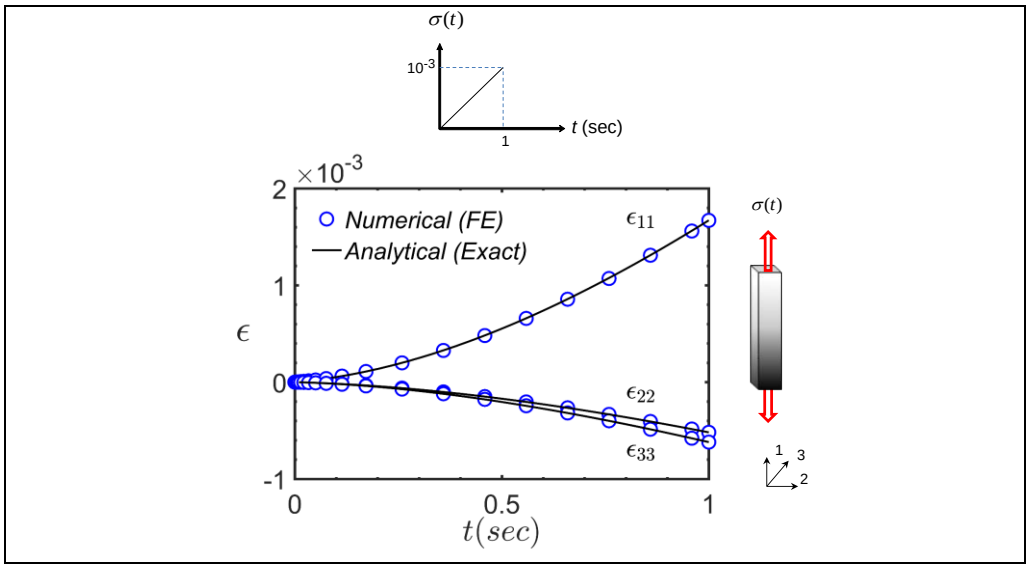

Figure 2: An orthotropic rod subjected to an applied uniaxial stress in the longitudinal direction, and free of stress in other directions [9]. Comparison of numerical predictions (using FE) and analytical solution for strains in the longitudinal and two transverse directions.

5 APPLICATION TO CREEP MODELLING OF PSL

There are many studies throughout the literature showing the time-dependent behaviour of both phenol formaldehyde (PF) resin and wood, especially at different moisture contents. One of the main applications of multi-scale modelling framework is predicting the response of strand-based wood composite structures. Strand-based composites are structural materials manufactured through combining orthotropic wood strands with small amount of adhesive (~5% by volume). The adhesive (e.g. a thermoset resin) glues the strands together. There are advantages associated with strand-based wood composites (e.g PSL) over solid wood [10]. The structural members made from these composites are often considered to be stronger, more reliable and more dimensionally stable than solid sawn lumber. The use of such structural composite lumber products as construction materials demands certain requirements of their mechanical properties be known such as stiffness and strength as well as some serviceability requirement such as the allowable amount of creep due to moisture, heat or long duration of loads (e.g. snow loads).

A numerical stochastic multi-scale modelling approach has been presented in [11] for predicting the elastic behaviour of PSL beams. Having developed a differential approach for orthotropic viscoelastic materials, the time-dependent behaviour of PSL beams subjected to a constant load can be simulated. In order to predict the creep of a PSL beam, a unit cell representing the microstructure of PSL which is consisting of resin and wood is employed for micro-mechanical simulations. It should be mentioned that both constituting phases (wood and resin) in PSL exhibit viscoelastic behaviour. However, for simplicity reasons, only the resin phase (PF) is considered to be viscoelastic and its behaviour is described with the viscoelastic parameters used in [12]. The three-dimensional orthotropic material constants for wood are average values for different pine species taken from [13] representing the actual PSL products.

In order to predict the creep response of the beams, the components of the unit cell effective relaxation matrix, $\overline{C}_{ij}$, are required. These can be estimated either analytically using the correspondence principle or numerically as described in [8]. Here, the numerical procedure presented in [8] was employed to derive components of the unit cell relaxation matrix. These components are required to characterize the viscoelastic behaviour of the material on the micro-scale. Variation of these components for fully bonded strands during time is shown in Figure 3.

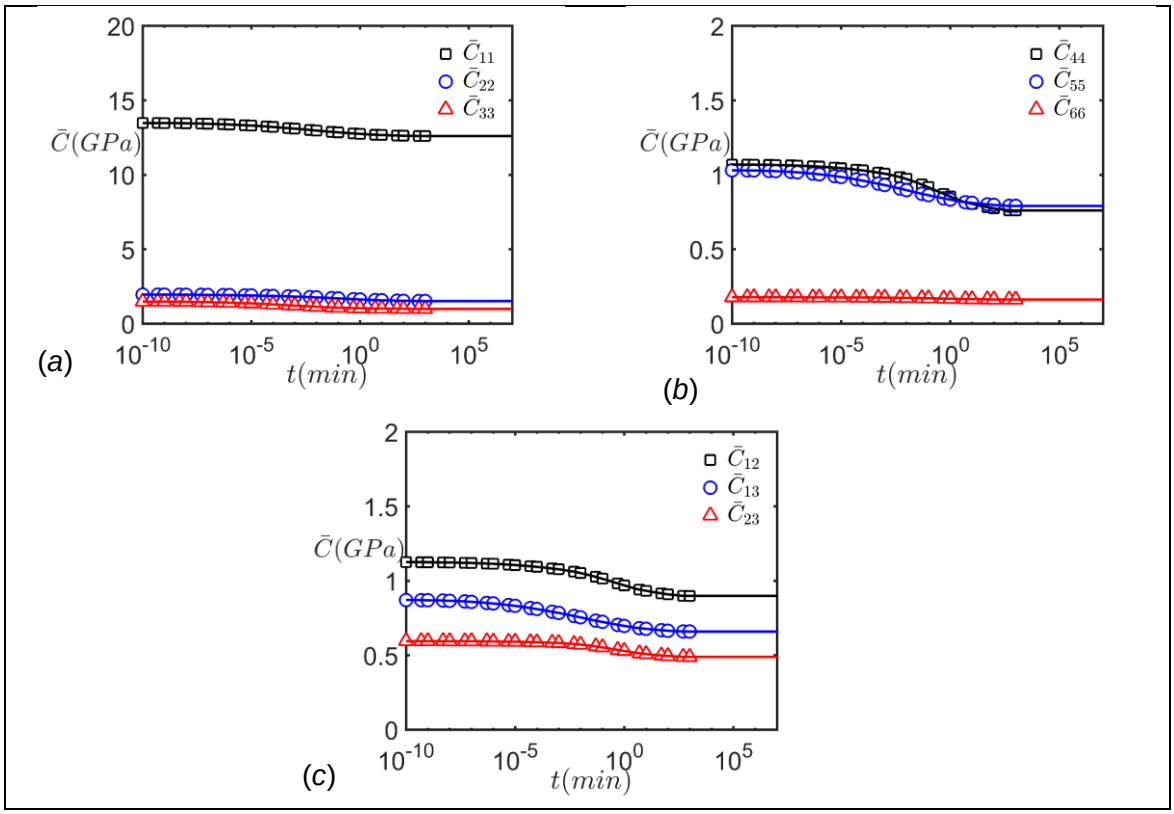

Figure 3: Variation of the effective relaxation matrix components $\bar{C}_{ij}$ versus time obtained from numerical analysis of PSL unit cell. Symbols denote numerical results and lines are the associated fitted curves.

In Figure 3, numerical results are shown with symbols while the fitted curves are plotted with lines. The differential approach for modelling the macroscopic behaviour of viscoelastic structures requires the components of relaxation matrix of the orthotropic material be defined by Prony series expansions following the formulation described in [8]. The unrelaxed and relaxed values and the Prony series parameters associated with each component are obtained from a curve fitting procedure on the numerical results. These parameters are given in Table 2 and Table 3 for reference.

Component	C_{ij}^{u} (GPa)	C_{ij}^{r} (GPa)
C_{11}	13.475	12.596
C_{22}	1.947	1.515
C_{33}	1.481	0.989
C_{44}	1.068	0.760
C_{55}	1.030	0.790
C_{66}	0.177	0.162
C_{12}	1.125	0.898
C_{13}	0.870	0.658
C_{23}	0.595	0.488

Table 2: Unrelaxed and relaxed values of components of the relaxation matrix for a PSL unit cell.

i	w_{11}	w_{22}	w_{33}	w_{44}	w_{55}	w_{66}	w_{12}	w_{13}	w_{23}	τ_i (min)
1	0.009	0.006	0.012	0.003	0.009	0.003	0.004	0.008	0.002	1.01E-09
2	0.018	0.012	0.024	0.007	0.017	0.007	0.008	0.017	0.003	1.01E-08
3	0.045	0.030	0.058	0.017	0.043	0.016	0.019	0.042	0.008	1.01E-07
4	0.056	0.037	0.072	0.022	0.053	0.022	0.024	0.052	0.012	1.01E-06
5	0.093	0.063	0.120	0.038	0.089	0.036	0.041	0.087	0.020	1.01E-05
6	0.110	0.078	0.139	0.052	0.106	0.050	0.055	0.104	0.033	1.01E-04
7	0.138	0.100	0.172	0.071	0.133	0.067	0.073	0.131	0.047	1.01E-03
8	0.154	0.137	0.171	0.131	0.152	0.120	0.125	0.152	0.112	1.01E-02
9	0.127	0.163	0.104	0.202	0.134	0.180	0.185	0.137	0.207	1.01E-01
10	0.124	0.186	0.070	0.232	0.133	0.240	0.230	0.136	0.273	1.01E+00
11	0.059	0.090	0.030	0.109	0.064	0.121	0.113	0.064	0.135	1.01E+01
12	0.065	0.098	0.030	0.115	0.069	0.137	0.123	0.069	0.148	1.01E+02

Table 3: Prony series parameters obtained from curve fitting of the numerical results.

Having characterized the viscoelastic behaviour of the material unit cell numerically (micro-mechanical step), the creep behaviour of the beam can now be determined from FE analysis of a beam consisting of several strands distributed within it (macro-mechanical step). PSL beams under three-point bending are analysed for this purpose. Each beam consists of 24 unit cells (strands with resin) arranged in a regular structure. The beam is assumed to have a square cross-section of 39 mm × 39 mm and a span of 380 mm between the supports as described in [14]. A constant distributed load with the total magnitude of 1.5 kN is applied at the centre of the beam on the top surface. The average displacement at the m centre nodes at the bottom surface of the beam is defined as follows:

$$\bar{\delta} = \frac{1}{m}\sum_{i=1}^{m}\delta_i \tag{15}$$

and recorded during time while the applied loads is maintained. The average displacement, $\bar{\delta}$, is used to construct deflection–time curves.

To evaluate the effect of strand orientation and resin area coverage of strands (i.e. voids), three cases are considered. In the first case, all strands are assumed to be fully bonded and aligned with the beam length. In the second case, random strand orientation is considered within each beam and is introduced by defining the material orientation within each unit cell making up the beam accordingly. For PSL beam consisting of random strands, strands are randomly distributed according to the orientation distribution described in [11] which is also given in figure below:

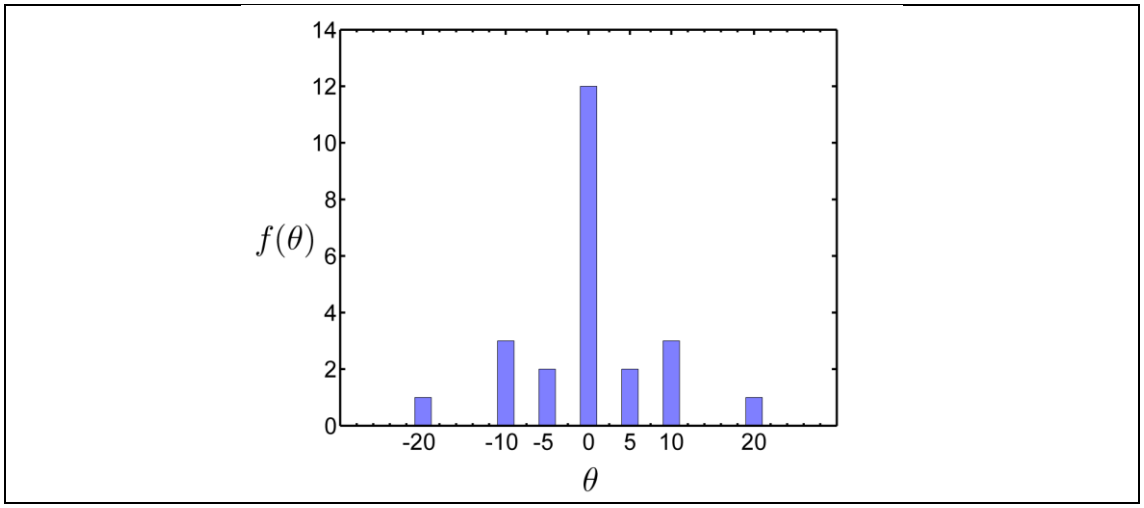

Figure 4: Strand orientation in the PSL beam consisting of random strands according to [11].

In order to investigate the effect of partial resin coverage of strands, voids are incorporated in the resin phase (20% by volume in the resin phase to represent 80% strand coverage by resin) according to [12] and considered as the third case.

A convergence study showed that a mesh size of 100 × 12 × 16 provides converged values for the node displacement on the bottom face of the beam in both cases. The results for the three PSL beams considered are presented in Figure 5.

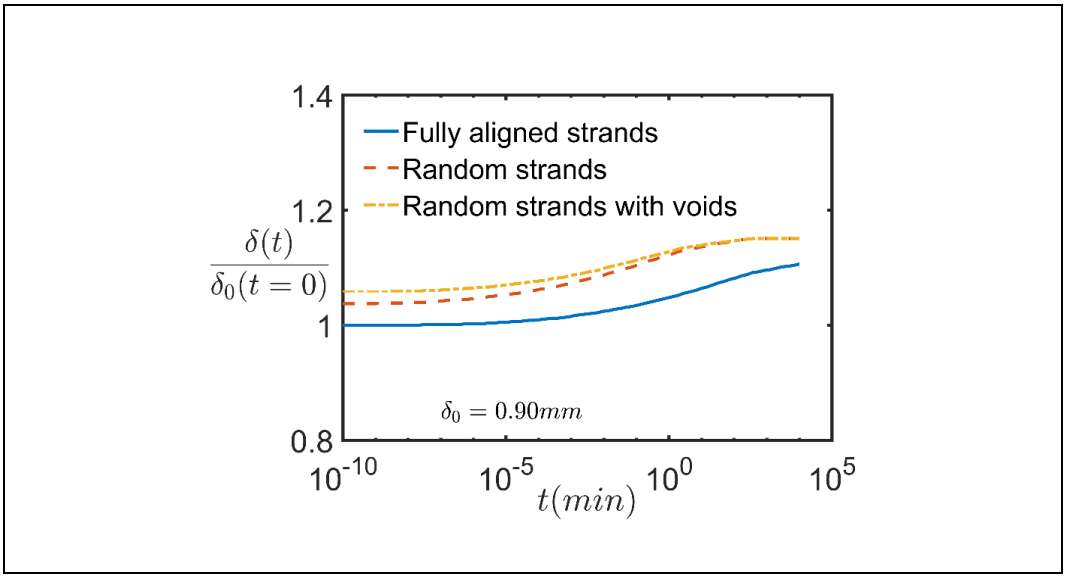

Figure 5: Creep curve for PSL beams consisting of aligned strands and random strands.

Note that the average deflection has been normalized by the initial elastic deflection of the beam consisting of aligned strands (0^o strands) in Figure 5. As it is expected, the PSL beam with fully bonded and aligned strands experiences lower deflections during time due to more contribution of elastic stiff strands. Figure 5 demonstrates the capability of the multi-scale framework in predicting viscoelastic behaviour of strand-based composite structures considering several variables including constituents' properties, microstructural features and geometrical parameters.

6 CONCLUSIONS

An efficient modelling strategy is presented for the analysis of viscoelastic composite structures. The presented approach enables engineers to simulate the viscoelastic behaviour of orthotropic composites that consist of at least one viscoelastic phase. Therefore, the time-dependent response of large complex structures to various loads at the macro-scale (e.g. meter level) can be predicted using the input parameters obtained from the output results of the micromechanical analyses at the micro-scale (e.g. mm level).

The modelling approach is specifically applied to predict the time-dependent behaviour of a special structural wood product, parallel strand lumber beam, subjected to a three-point bending load. As it is demonstrated, microstructural parameters (e.g. wood strand size and orientation distribution, as well as resin volume fraction and relaxation modulus) and their effect on the creep response of PSL can be considered using the developed approach. Results suggest that characterizing the correct viscoelastic behaviour of constituents (e.g. wood and resin) would enable future researchers to optimize the microstructure of structural composites for specific load scenarios.

7 ACKNOWLEDGEMENTS

The authors would like to thank the Natural Sciences and Engineering Research Council of Canada (NSERC) for their financial support of this research. The authors are also grateful to the insights provided by Professors Anoush Poursartip and Fernand Ellyin from UBC, Professor Carole Nadot-Marin from Institut Pprime (France) during various research discussions held at UBC.

REFERENCES

[1] P. Kanouté, D. P. Boso, J. L. Chaboche, and B. A. Schrefler, “Multiscale Methods for Composites: A Review,” *Arch Comput Methods Eng*, vol. 16, pp. 31–75, 2009.

[2] M. G. D. Geers, V. G. Kouznetsova, and W. A. M. Brekelmans, “Multi-scale computational homogenization: Trends and challenges,” *J. Comput. Appl. Math.*, vol. 234, no. 7, pp. 2175–2182, 2010.

[3] R. Christensen, *Theory of viscoelasticity: an introduction*. New York: Academic Press Inc., 1982.

[4] N. Zobeiry, “Viscoelastic constitutive models for evaluation of residual stresses in thermoset composites during cure.” 2006.

[5] A. Matzenmiller and S. Gerlach, “Micromechanical modeling of viscoelastic composites with compliant fiber-matrix bonding,” *Comput. Mater. Sci.*, vol. 29, no. 3, pp. 283–300, 2004.

[6] N. Zobeiry, S. Malek, R. Vaziri, and A. Poursartip, “A differential approach to finite element modelling of isotropic and transversely isotropic viscoelastic materials,” *Mech. Mater.*, vol. 97, pp. 76–91, 2016.

[7] N. Zobeiry, R. Vaziri, and A. Poursartip, “Differential implementation of the viscoelastic response of a curing thermoset matrix for composites processing,” *J. Eng. Mater. Technol. Asme*, vol. 128, no. 1, pp. 90–95, Jan. 2006.

[8] S. Malekmohammadi, “Efficient multi-scale modelling of viscoelastic composites with different microstructures,” The University of British Columbia, 2014.

[9] H. Poon and M. F. Ahmad, “A material point time integration procedure for anisotropic, thermo rheologically simple, viscoelastic solids,” *Comput. Mech.*, vol. 21, no. 3, pp. 236–242, Apr. 1998.

[10] K. J. Fridley, “Wood and wood-based materials: current status and future of a structural material,” *J. Mater. Civ. Eng.*, vol. 14, no. 2, pp. 91–96, 2002.

[11] T. Gereke *et al.*, “Multiscale Stochastic Modeling of the Elastic Properties of Strand-Based Wood Composites,” *J. Eng. Mech.*, pp. 791–799, 2012.

[12] S. Malekmohammadi, B. Tressou, C. Nadot-Martin, F. Ellyin, and R. Vaziri, “Analytical micromechanics equations for elastic and viscoelastic properties of strand-based composites,” *J. Compos. Mater.*, vol. 48, no. 15, pp. 1857–1874, 2014.

[13] Forest Products Laboratory - USDA, *Wood Handbook: Wood as an Engineering Material*, vol. General Te. 2010.

[14] S. Arwade, P. Clouston, and R. Winans, “Measurement and Computational Modeling of the Mechanical Properties of Parallel Strand Lumber,” *J. Eng. Mech.*, vol. 135, no. 9, pp. 897–905, 2014.